Hepatic inactivation of murine *Surf4* results in marked reduction in plasma cholesterol

Vi T. Tang[1,2], Joseph McCormick[2], Bolin Xu[3], Yawei Wang[4], Huan Fang[3], Xiao Wang[3,5], David Siemieniak[2,10], Rami Khoriaty[6,7], Brian T. Emmer[6], Xiao-Wei Chen[5], David Ginsburg[2,6,8-10]

[1]Department of Molecular and Integrative Physiology, University of Michigan, Ann Arbor, MI

[2]Life Sciences Institute, University of Michigan, Ann Arbor, MI

[3]College of Future Technology, Peking University, Beijing 100871, China

[4]Center for Life Sciences, Peking University, Beijing 100871, China

[5]State Key Laboratory of Membrane Biology, Peking University, Beijing 100871, China

[6]Department of Internal Medicine, University of Michigan, Ann Arbor, MI

[7]Department of Cell and Developmental Biology, University of Michigan, Ann Arbor, MI

[8]Department of Human Genetics, University of Michigan, Ann Arbor, MI

[9]Department of Pediatrics and Communicable Diseases, University of Michigan, Ann Arbor, MI

[10]Howard Hughes Medical Institute, University of Michigan, Ann Arbor, MI

Short title: Hepatic SURF4 inactivation lowers plasma cholesterol

Correspondence: David Ginsburg (ginsburg@umich.edu)

Room 5028

Life Sciences Institute

210 Washtenaw Avenue

Ann Arbor, MI 48109-2216

Abstract

PCSK9 negatively regulates low-density lipoprotein receptor (LDLR) abundance on the cell surface, leading to decreased hepatic clearance of LDL particles and increased levels of plasma cholesterol. We previously identified SURF4 as a cargo receptor that facilitates PCSK9 secretion in HEK293T cells (Emmer et al., 2018). Here, we generated hepatic SURF4-deficient mice (*Surf4*$^{fl/fl}$ *Alb-Cre*$^{+}$) to investigate the physiologic role of SURF4 *in vivo*. *Surf4*$^{fl/fl}$ *Alb-Cre*$^{+}$ mice exhibited normal viability, gross development, and fertility. Plasma PCSK9 levels were reduced by ~60% in *Surf4*$^{fl/fl}$ *Alb-Cre*$^{+}$ mice, with a corresponding ~50% increase in steady state LDLR protein abundance in the liver, consistent with SURF4 functioning as a cargo receptor for PCSK9. Surprisingly, these mice exhibited a marked reduction in plasma cholesterol and triglyceride levels out of proportion to the partial increase in hepatic LDLR abundance. Detailed characterization of lipoprotein metabolism in these mice instead revealed a severe defect in hepatic lipoprotein secretion, consistent with prior reports of SURF4 also promoting the secretion of apolipoprotein B. Despite a small increase in liver mass and lipid content, histologic evaluation revealed no evidence of steatohepatitis or fibrosis in *Surf4*$^{fl/fl}$ *Alb-Cre*$^{+}$ mice. Acute depletion of hepatic SURF4 by CRISPR/Cas9 or liver-targeted siRNA in adult mice confirms these findings. Together, these data support the physiologic significance of SURF4 in the hepatic secretion of PCSK9 and APOB-containing lipoproteins and its potential as a therapeutic target in atherosclerotic cardiovascular diseases.

Introduction

An elevated plasma level of low-density lipoprotein (LDL) is a major risk factor for atherosclerotic cardiovascular disease (Chapman et al., 2011), which is the leading cause of death worldwide. LDL is derived in the circulation by processing of very-low-density lipoprotein (VLDL) particles, which is synthesized and secreted by the liver. In humans, the major protein component of VLDL is APOB100, which is cotranslationally lipidated in the endoplasmic reticulum (ER) (Kolovou et al., 2015). LDL is cleared from circulation by the LDL receptor (LDLR) on cell surfaces. Proprotein convertase subtilisin/kexin type 9 (PCSK9) is a soluble protein that is secreted by the liver and negatively regulates LDLR abundance by inducing its degradation (Benjannet et al., 2004).

Proteins destined for extracellular secretion are transported from the endoplasmic reticulum (ER) to Golgi by COPII coated vesicles/tubules (Bonifacino & Glick, 2004; Palade, 1975). SEC24 is a key component of the COPII inner coat, which appears to play a primary role in selecting cargo proteins for export from the ER (Miller et al., 2002). The mammalian genome encodes 4 paralogs of *Sec24* (*Sec24a-d*) (Wendeler et al., 2007). Mice genetically deficient in SEC24A exhibit moderate hypocholesterolemia due to a selective block in PCSK9 secretion from the ER, resulting in an ~50% reduction in plasma PCSK9 levels (Chen et al., 2013).

We previously reported a whole genome CRISPR screen in HEK293T cells heterologously expressing PCSK9, identifying Surfeit locus protein 4 (SURF4) as the putative cargo receptor potentially linking PCSK9 within the ER lumen to SEC24A on the cytoplasmic face of the ER membrane (Emmer et al., 2018). SURF4 is a 29 kDa protein with multiple transmembrane domains that localize to the ER and ER-Golgi intermediate compartment (ERGIC) (Mitrovic et al., 2008). *SURF4* is a homolog of *Erv29p,* a well-characterized cargo receptor in yeast that mediates the ER to Golgi trafficking of pro-α-mating factor (Belden, 2001). The SURF4 ortholog

in *C. elegans*, SFT-4, controls the ER export of the yolk protein VIT-2 (Saegusa et al., 2018). Recent studies in human cells have also implicated SURF4 in the trafficking of other cargoes, including apolipoprotein B (APOB) (Emmer et al., 2020; Saegusa et al., 2018; B. Wang et al., 2021), erythropoietin (EPO) (Lin et al., 2020), growth hormone, dentin sialophosphoprotein, and amelogenin (Yin et al., 2018). A role for SURF4 in APOB secretion was further supported by a recent study in which acute deletion of hepatic *Surf4* in adult mice caused hypocholesterolemia and a reduction in hepatic lipoprotein secretion (X. Wang et al., 2021).

To investigate the physiologic significance of SURF4 in the secretion of PCSK9 and other putative cargoes, we previously generated mice with germline deletion of *Surf4*, which resulted in early embryonic lethality (Emmer et al., 2020). We now report the generation and characterization of mice with *Surf4* selectively inactivated in the liver by combining a conditional *Surf4* allele (*Surf4*^{fl}) with a Cre recombinase expressed under the control of the albumin promoter (*Alb-Cre*). *Surf4*$^{fl/fl}$ *Alb-Cre*$^{+}$ mice exhibit normal development, survival and fertility, with marked plasma hypocholesterolemia associated with a hepatic secretion defect for PCSK9 and APOB-containing lipoproteins without evidence for liver injury. Acute inactivation of hepatic *Surf4* by CRISPR/Cas9 or liver-targeted siRNA in adult mice further confirms these findings and the potential of hepatic SURF4 as a therapeutic target in atherosclerotic cardiovascular disease.

Results

Liver-specific deletion of *Surf4* is compatible with normal development and survival in mice

To investigate long term *Surf4* inactivation in hepatocytes *in vivo*, we generated mice with the *Surf4* gene genetically inactivated specifically in the liver by combining a previously reported conditional *Surf4* allele (in which *Surf4* exon 2 is flanked by loxP sites, denoted *Surf4*^{fl}) (X. Wang et al., 2021) with a *Cre* recombinase transgene under control of the *Albumin* promoter

(*Alb-Cre*). *Surf4*$^{fl/fl}$ *Alb-Cre*$^{+}$ mice were observed at the expected Mendelian ratio (**Table 1**). Both male and female *Surf4*$^{fl/fl}$ *Alb-Cre*$^{+}$ mice were fertile and produce offspring of the predicted genotypes at expected Mendelian ratios (**Table 1**).

Excision of exon 2 is predicted to result in a frameshift mutation and the generation of a premature termination codon 8 base pairs downstream of the new exon1-3 junction (**Fig. 1A**). Analysis of genomic DNA collected from mouse tails and livers of *Surf4*$^{fl/fl}$ *Alb-Cre*$^{+}$ mice demonstrated efficient Cre-mediated excision of *Surf4* exon 2 only in the liver (**Fig. 1B**), with the level of exon 2 containing *Surf4* transcripts in *Surf4*$^{fl/fl}$ *Alb-Cre*$^{+}$ livers reduced to ~5% of controls (**Fig. 1C**). This residual unexcised *Surf4* mRNA is likely derived from nonhepatocyte cell types in the liver. Quantitative PCR of liver cDNA using primers outside of exon 2 demonstrated a 38% reduction in total *Surf4* mRNA transcript in *Surf4*$^{fl/fl}$ *Alb-Cre*$^{+}$ mice compared to *Surf4*$^{fl/fl}$ *Alb-Cre*$^{-}$ littermates, likely due to nonsense mediated mRNA decay (Popp & Maquat, 2013). Analysis of *Surf4* mRNA transcripts by RNA sequencing confirmed the expected reduction of reads spanning the exon 1-2 and exon 2-3 junctions in *Surf4*$^{fl/fl}$ *Alb-Cre*$^{+}$ livers compared to controls (150 and 148 versus 2623 and 2490 reads, respectively, **Fig. 1D** and **Fig. S1**). Consistent with the qPCR data and incomplete nonsense mediated mRNA decay, we identified 928±51 reads mapping to the exon1-exon3 junction of the *Surf4* mRNA in liver from *Surf4*$^{fl/fl}$ *Alb-Cre*$^{+}$ mice and zero in *Surf4*$^{fl/fl}$ *Alb-Cre*$^{-}$ samples (**Fig. S.1**). This residual exon 2 excised mRNA in *Surf4*$^{fl/fl}$ *Alb-Cre*$^{+}$ liver contains a premature stop codon near the start of the SURF4 coding sequence (codon 23 of 270), which is expected to be translated into a nonfunctional, truncated protein (**Fig. 1A**).

We also detected 404±39 reads (none in controls) mapping to the exon1-4 junction of an alternatively spliced *Surf4* mRNA in *Surf4*$^{fl/fl}$ *Alb-Cre*$^{+}$ samples (**Fig. 1D**). Exclusion of exon 2 and 3 is predicted to restore the reading frame and result in the production of an internally

deleted SURF4, missing ~1/3 of the full length sequence (**Fig. 1A)**. Though also likely to be nonfunctional, residual activity and/or a dominant-negative effect of this internally deleted SURF4 cannot be excluded.

Reduced circulating PCSK9 and increased LDLR levels in *Surf4$^{fl/fl}$ Alb-Cre^{+}* mice

We previously demonstrated a key role of SURF4 in the efficient trafficking of PCSK9 heterologously expressed in HEK293T cells (Emmer et al., 2018). To test the dependence of PCSK9 secretion on SURF4 *in vivo*, we first examined steady state serum PCSK9 levels in *Surf4$^{fl/fl}$ Alb-Cre^{+}* and *Surf4$^{fl/fl}$ Alb-Cre^{-}* control mice. Serum PCSK9 levels were reduced by ~60% in *Surf4$^{fl/fl}$ Alb-Cre^{+}* compared to *Surf4$^{fl/fl}$ Alb-Cre^{-}* mice (from 46.0±19.0 ng/mL to 17.8±6.42 ng/mL, **Fig. 2A**), though PCSK9 accumulation was not observed in liver lysates (**Fig. 2B-C**). Quantitative RT-PCR revealed that *Pcsk9* mRNA levels were also unchanged (**Fig. S.2**), consistent with a defect in PCSK9 protein secretion rather than gene expression as the cause for decreased plasma PCSK9 levels.

In contrast to the above findings, Wang et al reported no change in plasma PCSK9 levels in *Surf4$^{fl/fl}$ Alb-Cre^{+}* mice (B. Wang et al., 2021). To address this issue, and to exclude complex adaptation to hepatic SURF4 deletion induced *in utero*, we acutely inactivated hepatic *Surf4* in adult mice using a previously reported Cas9 mouse system (X. Wang et al., 2021). Analyses utilizing 3 different *Surf4* targeting sgRNAs demonstrated a reproducible ~40% reduction in plasma PCSK9 levels for all mice receiving *Surf4* targeting sgRNA compared to control mice (**Fig. 2D**), consistent with our findings in *Surf4$^{fl/fl}$ Alb-Cre^{+}* mice.

Since PCSK9 is a negative regulator of LDLR, we next quantified LDLR levels in liver lysates collected from control and *Surf4$^{fl/fl}$ Alb-Cre^{+}* mice. As shown in **Fig. 2E-F**, *Surf4$^{fl/fl}$ Alb-Cre^{+}* mice

exhibit an ~1.5-fold increase in LDLR abundance in liver lysates compared to controls, consistent with the observed ~60% reduction in circulating PCSK9 level.

Marked reduction of plasma cholesterol in *Surf4$^{fl/fl}$ Alb-Cre^{+}* mice

Humans with heterozygous loss of function mutations in *PCSK9* exhibit an ~40% reduction in circulating cholesterol (Cohen et al., 2005) with a similar reduction observed in *Pcsk9$^{+/-}$* mice (Rashid et al., 2005). Though *Surf4$^{fl/fl}$ Alb-Cre^{+}* mice exhibit similar reductions in PCSK9, total serum cholesterol is markedly reduced (from 54.3±15.1 mg/dL in *Surf4$^{fl/fl}$ Alb-Cre^{-}* mice to 9.51±2.6 mg/dL in *Surf4$^{fl/fl}$ Alb-Cre^{+}* mice) (**Fig. 2G**). No change in cholesterol was observed in the limited numbers of mice haploinsufficient for *Surf4* in the liver (*Surf4^{fl+l} Alb-Cre^{+}*). Analysis of fractionated pooled sera demonstrated marked reductions in cholesterol and triglyceride content in *Surf4$^{fl/fl}$ Alb-Cre^{+}* mice among all 3 major classes of lipoproteins – very low density lipoprotein (VLDL), low density lipoprotein (LDL), and high density lipoprotein (HDL) (**Fig. 2H**). This striking hypocholesterolemia phenotype is sustained through at least 1 year of age (**Fig. S.3B**), with no difference in body mass between *Surf4$^{fl/fl}$ Alb-Cre^{-}* and *Surf4$^{fl/fl}$ Alb-Cre^{+}* littermates (**Fig. S.3A** and **S.3C**).

Consistent with a role of SURF4 in the ER export of APOB-containing lipoproteins (X. Wang et al., 2021), the mean serum APOB level in fasted *Surf4$^{fl/fl}$ Alb-Cre^{+}* mice was 3.88±2.63 mg/mL, a >98% reduction compared to *Surf4$^{fl/fl}$ Alb-Cre^{-}* mice (300±157mg/mL, **Fig. 3A**). Western blotting demonstrated a trend towards an accumulation of APOB in the livers of *Surf4$^{fl/fl}$ Alb-Cre^{+}* mice compared to littermate controls, predominantly in an endoglycosidase H (endo H) sensitive form (**Fig. 3B-C)**, indicative of ER retention (Freeze & Kranz, 2010).

We next examined hepatic triglyceride secretion in *Surf4$^{fl/fl}$ Alb-Cre^{+}* and control mice. For this experiment, mice were fasted to remove intestinal absorption of dietary fat and tissue lipid

uptake was blocked by administration of a lipoprotein lipase inhibitor, with liver triglyceride output subsequently monitored by sampling of plasma triglycerides over 24 hours. Following fasting and inhibition of triglyceride hydrolysis, blood glucose levels fell equivalently between *Surf4*$^{fl/fl}$ *Alb-Cre*$^{+}$ and *Surf4*$^{fl/fl}$ *Alb-Cre*$^{-}$ littermates (**Fig. 3D**). Although serum cholesterol and triglyceride levels steadily increased in both groups over time, both levels were consistently and significantly lower in *Surf4*$^{fl/fl}$ *Alb-Cre*$^{+}$ mice compared to littermate controls (**Fig. 3E-F**). Following an initial decrease in the first hour after lipoprotein lipase inhibition, serum APOB levels steadily rose in control mice (**Fig. 3G)**. In contrast, serum APOB levels were markedly reduced at baseline in *Surf4*$^{fl/fl}$ *Alb-Cre*$^{+}$ mice, and showed minimal increase after lipoprotein lipase inhibition.

Intestinal lipid absorption and tissue lipid uptake are unaffected in *Surf4*$^{fl/fl}$ *Alb-Cre*$^{+}$ mice

To assess the potential role of hepatic *Surf4* gene expression on dietary lipid absorption, mice were fed a ^{3}H triolein-labelled lipid load following an overnight fast. No significant differences in blood glucose, serum triglycerides, non-esterified fatty acids, or total intestinal uptake of dietary lipids were observed between control and *Surf4*$^{fl/fl}$ *Alb-Cre*$^{+}$ mice (**Fig. 4A-D**). Similarly, no significant differences were observed in tissue lipid uptake or fatty acid oxidation between *Surf4*$^{fl/fl}$ *Alb-Cre*$^{+}$ mice and littermate controls (**Fig. 4E-F**).

Loss of liver *Surf4* expression results in mild lipid accumulation but no steatohepatitis or fibrosis

Surf4$^{fl/fl}$ *Alb-Cre*$^{+}$ mice exhibited mildly enlarged livers (**Fig. 5A**), with a small increase in hepatic fat content and a reduction in lean mass compared to littermate controls (**Fig. 5B**). However, no differences were observed in fasting hepatic cholesterol, triglyceride, phospholipid, or nonesterified fatty acid content (**Fig. 5C**). Hepatic lipid accumulation can lead to steatohepatitis and liver damage (Ipsen et al., 2018). However, at 8-12 week of age, serum albumin, bilirubin,

and liver function markers were indistinguishable between *Surf4*$^{fl/fl}$ *Alb-Cre*$^{+}$ and control mice (**Fig. S.4** and **Fig. 5D**) and histologic analyses detected no evidence for steatohepatitis or fibrosis (**Fig. 5E**). Finally, deep sequencing of liver mRNA identified only limited gene expression changes in response to *Surf4* deletion (**Fig. 5F**). Significant downregulation was observed for several genes involved in fatty acid biosynthesis processes (**Fig. 5H**). The most significantly upregulated gene in *Surf4*$^{fl/fl}$ *Alb-Cre*$^{+}$ liver was *Derl3*, a component of the ERAD pathway, which could be induced by protein accumulation in the ER of *Surf4*$^{fl/fl}$ *Alb-Cre*$^{+}$ mice. Genes involved in the unfolded protein response, such as *Ire1*, *Aft6*, and *Perk* (Hetz et al., 2020), were not upgregulated in *Surf4*$^{fl/fl}$ *Alb-Cre*$^{+}$ mice (**Fig. 5F**).

Dose-dependent reduction of plasma lipids in response to depletion of SURF4 by siRNA

To confirm the profound hypocholesterolemia with few adverse consequences observed in *Surf4*$^{fl/fl}$ *Alb-Cre*$^{+}$ mice, and to further explore SURF4 inhibition as a potential therapeutic approach, we next tested depletion of hepatic SURF4 using liver-targeted siRNA in adult mice. Mice were treated with control or *Surf4* targeting siRNA at multiple doses between 0.5-4 mg/kg. Mice treated with *Surf4* targeting siRNA demonstrated a dose-dependent reduction of liver *Surf4* mRNA and protein levels (**Fig. 6A** and **Fig. S.4**). As expected, plasma PCSK9, cholesterol, triglycerides, APOB, and APOA1 levels were inversely correlated with siRNA dosage, with the highest siRNA dose (4 mg/kg) resulting in cholesterol levels similar to those observed in *Surf4*$^{fl/fl}$ *Alb-Cre*$^{+}$ mice (**Fig. 6B-D** and **Fig. S4**). Finally, no differences in plasma ALT and AST levels were observed between control and siRNA treated mice, suggesting that siRNA treatment and *Surf4* depletion does not lead to liver injury, even at the highest siRNA dose (**Fig. 6E-F**).

Discussion

We found that embryonic deletion of *Surf4* in hepatocytes results in profound hypocholesterolemia in mice associated with impaired hepatic lipoprotein secretion and normal

dietary fat absorption. In addition, we also demonstrated that plasma PCSK9 levels are reduced in *Surf4*$^{fl/fl}$ *Alb-Cre*$^{+}$ mice. Hepatocyte specific *Surf4* deletion was well tolerated, with only modest increases in hepatic mass and lipid content, and no evidence of hepatic dysfunction or steatohepatitis. Finally, we confirm these findings by siRNA depletion of hepatic SURF4 in adult mice, which leads to reductions of plasma cholesterol, triglycerides, and PCSK9 in a dose dependent manner without apparent deleterious consequences in the liver.

We previously reported that PCSK9 is dependent on SURF4 for efficient secretion in cultured HEK293T cells (Emmer et al., 2018). In contrast, Shen et al reported that depletion of SURF4 by siRNA in cultured human hepatocytes leads to increased *Pcsk9* gene expression resulting in increased rather than decreased PCSK9 secretion (Shen et al., 2020). The same group also recently reported analysis of *Surf4*$^{fl/fl}$ *Alb-Cre*$^{+}$ mice, observing no change in plasma PCSK9 levels, in contrast to our findings in a similar genetic model. Our current findings, using three independent mouse models, are consistent with our previous *in vitro* data and support a physiologic role for SURF4 in facilitating the efficient transport of PCSK9 (as well as APOB) through the secretory pathway. The decrease in plasma PCSK9 in *Surf4*$^{fl/fl}$ *Alb-Cre*$^{+}$ mice is similar to that observed in SEC24A-deficient mice (Chen et al., 2013). Additionally, we also detected a 1.5 fold increase in LDLR level in liver lysates collected from *Surf4*$^{fl/fl}$ *Alb-Cre*$^{+}$ mice, consistent with the reduction in circulating PCSK9. The increased hepatocyte LDLR levels in *Surf4*$^{fl/fl}$ *Alb-Cre*$^{+}$ mice are not accompanied by upregulation of *Ldlr* mRNA as measured by RNA-seq analysis, consistent with the increase in LDLR abundance being mediated by PCSK9 activity rather than an increase in gene expression. Furthermore, a recent report by Gomez-Navarro et al independently demonstrated that PCSK9 relies on both SEC24A and SURF4 for secretion and that chemical disruption of SEC24A-SURF4 interaction is sufficient to reduce PCSK9 secretion (Gomez-Navarro et al., 2022). Taken together, these data are consistent with the proposed function of SURF4 as a cargo receptor linking PCSK9 in the ER lumen to the

SEC24A component of the COPII coat on the cytoplasmic face of the ER (Emmer et al., 2018). The basis for the discrepancy between our findings and those of B. Wang and colleagues (B. Wang et al., 2021) is unclear but may be related to differences in mouse genetic or husbandry (Tang et al., 2017), or to technical differences in PCSK9 quantification.

The profound hypocholesterolemia we observed in *Surf4*$^{fl/fl}$ *Alb-Cre*$^{+}$ mice is in agreement with two other studies in which hepatic *Surf4* was acutely inactivated using an AAV/Cas9 mouse system (X. Wang et al., 2021) or a similar *Surf4*$^{fl/fl}$ and *Alb-Cre* model (B. Wang et al., 2021). We also confirmed this observation in a third model using siRNA mediated knockdown of *Surf4* transcripts in mouse livers. The decrease in circulating cholesterol is likely due to impaired secretion of APOB containing lipoprotein particles from the liver, and is consistent with multiple previous reports suggesting that APOB is a cargo for SURF4 (Emmer et al., 2020; Saegusa et al., 2018; B. Wang et al., 2021; X. Wang et al., 2021). Despite remarkably low plasma cholesterol levels, *Surf4*$^{fl/fl}$ *Alb-Cre*$^{+}$ mice exhibit normal growth and fertility compared to littermate controls. Plasma cholesterol is an important precursor for steroid hormone synthesis. However, given that both male and female *Surf4*$^{fl/fl}$ *Alb-Cre*$^{+}$ mice are fertile, it is unlikely that sex hormone synthesis is significantly perturbed in these mice. Consistent with this conclusion, Chang et al recently reported that even though lipid droplets and cholesterol are depleted in the adrenal glands of *Surf4*$^{fl/fl}$ *Alb-Cre*$^{+}$ mice, circulating adrenal steroid hormone levels are unchanged under resting and stressed conditions (Chang et al., 2021).

Impaired protein secretion could lead to accumulation of proteins in the ER lumen, potentially triggering activation of UPR pathways and induction of ERAD. Indeed, livers from *Surf4*$^{fl/fl}$ *Alb-Cre*$^{+}$ mice exhibited upregulation of mRNA for *Derl3*, an ER transmembrane protein that is a functional component of the ER-associated degradation (ERAD) complex (Oda et al., 2006). While *Derl3* is thought to be a target of the IRE1-XBP1 pathway, we did not detect upregulation

of *Ire1* or *Xbp1*, or other ERAD components at the mRNA levels in *Surf4*$^{fl/fl}$ *Alb-Cre*$^{+}$ mice. Instead upregulation of *Derl3* could be an adaptive response to the protein accumulation in the ER leading to the rapid degradation of these proteins. This can also explain the lack of liver PCSK9 accumulation and a mild increase in liver APOB levels (relative to a significant reduction of plasma levels) in *Surf4*$^{fl/fl}$ *Alb-Cre*$^{+}$ mice.

Recently, Musunuru et al reported that *in vivo* CRISPR-mediated base editing of hepatic *PCSK9* leads to an ~60% reduction in plasma cholesterol in cynomolgus monkeys without overt hepatotoxicity (Musunuru et al., 2021). Our data suggest that hepatic *Surf4* could be similarly targeted, potentially achieving an even more profound reduction in plasma cholesterol without deleterious consequences. Indeed, it has been shown that inactivation of hepatic *Surf4* is protective against diet-induced atherosclerosis in mice with PCSK9 overexpression (X. Wang et al., 2021), LDLR deficiency (B. Wang et al., 2021), and APOE deficiency (Shen et al., 2022). Furthermore, polymorphism and mild reduction of *SURF4* expression strongly associate with lower plasma lipid levels and reduced risks of cardiovascular disease in human populations (X. Wang et al., 2021). Here, we further demonstrate that even more modest reductions in SURF4 induced by siRNA targeting are likely to confer significant lipid-lowering, though such benefits must be weighed against potential toxicity from disrupting the secretion of other SURF4-dependent cargoes.

Materials and Methods

Animal care and use

All animal care and use complied with the Principles of Laboratory and Animal Care established by the National Society for Medical Research. All animal protocols in this study have been approved by the Institutional Animal Care and Use Committee (IACUC) of the University of

Michigan (protocol number PRO00009304) and the IACUC of Peking University. Both male and female mice were used in this study unless otherwise specified.

Generation of conditional *Surf4* knockout mice

The generation of mice carrying a conditional *Surf4* allele in which exon 2 of the gene is flanked by 2 loxP sites (*Surf4*^{fl}) has been previously described (X. Wang et al., 2021). *Surf4*$^{fl/+}$ mice were crossed with mice carrying an *Alb-Cre* transgene (Adams et al., 2014) to obtain *Surf4*$^{fl/+}$ *Alb-Cre*$^{+}$ mice. These mice were then crossed to *Surf4*$^{fl/fl}$ mice to generate *Surf4*$^{fl/fl}$ *Alb-Cre*$^{+}$ mice. The *Surf4*^{fl} and *Alb-Cre* alleles were maintained on the C57BL/6J background by continuous backcrosses to C57BL/6J mice (0006640, Jackson Laboratory, Bar Harbor ME).

Genotyping assays

Tail clips were obtained from 2 weeks old mice for genomic DNA isolation and genotyping. PCR was performed using Go-Taq Green Master Mix (Promega, Madison, WI) and resulting products were resolved by 3% agarose gel electrophoresis. All primers used for genotyping are listed in **Table S.1**. Those used for genotyping the *Surf4* locus are also depicted in **Fig. 1A**. For the *Alb-Cre* transgene, parental mice were genotyped using promoter-specific *Cre* primers and offspring were genotyped with primers that detect the *Cre* transgene (**Table S.1**).

Blood and tissue collection

Mice were fasted overnight for up to 16 hours prior to sample collection. For non-terminal experiments, blood was collected from the superficial temporal vein using a 4 mm sterile lancet. For terminal experiments, mice were first euthanized by isoflurane inhalation and blood was drawn from the inferior vena cava using a 23G needle and a 1 ml syringe. Blood was collected into a serum separator tube (365967, BD, Franklin Lakes NJ), allowed to clot at room temperature for at least 10 minutes, and centrifuged at 15,000 g for 10 minutes to separate

serum. Sera were aliquoted and stored at -80°C. Liver tissue were collected as previously described (Emmer et al., 2020).

Analysis for sera from *Surf4* liver knockout mice

Sera were analyzed by a colorimetric assay for total cholesterol (SB-1010-225, Fisher Scientific, Hampton NH) and by ELISAs for PCSK9 (MPC900, R&D Systems, Minneapolis MN) and APOB (ab230932, Abcam, Cambridge UK). Serum lipoprotein fractionation assays were performed at the University of Cincinnati Mouse Metabolic Phenotyping Center. Sera were pooled from 5 mice for each genotype and fractionated by fast liquid protein chromatography (FPLC) into 50 fractions. Cholesterol (NC9343696, Fisher, Hampton NH) and triglyceride (TR213, Randox Laboratories, Crumlin UK) content in each fraction were determined using a microliter plate enzyme-based assay. Liver function tests were performed at the University of Michigan In-Vivo Animal Core (IVAC) with sera collected from individual mice using a Liasys analyzer (AMS Alliance).

Hepatic lipoprotein secretion assay

Hepatic triglyceride secretion assays were performed at the University of Michigan Mouse Metabolic Phenotyping Center as previously described (Millar et al., 2005). Blood levels of glucose were measured using a glucometer (Acucheck, Roche, Basel Switzerland) and plasma levels of cholesterol (SB-1010-225, Fisher Scientific, Hampton NH) and triglycerides (10010303, Cayman Chemical, Ann Arbor MI) were determined using colorimetric assay kits. Plasma APOB levels were determined by ELISA (ab230932, Abcam, Cambridge UK).

Oral fat tolerance test and lipid flux assay

Oral fat tolerance test and lipid flux assay were performed at the University of Michigan Mouse Metabolic Phenotyping Center. Mice were fasted overnight and ^{3}H triolein-labeled olive oil

(0.026 µCi/µl) was given via oral gavage at 5 µl/g of body mass. Blood samples were collected at time 0, 30, 60, 120, and 240 minutes after the gavage via tail vein bleeding. Plasma levels of triglyceride (10010303, Cayman Chemical, Ann Arbor MI) and non-esterified fatty acid (NEFA-HR (H2), Wako Pure Chemical Industries, Ltd, Richmond VA) were determined using the colorimetric assays. Plasma radioactivity, reported as ^{3}H disintegration per minute (dpm), were determined from 2 µl of serum at each time point.

Tissues samples (liver, heart, gastrocnemius muscle, and perigonadal fat) were collected at the 240 minute time point, flash frozen in liquid nitrogen and stored at -80ºC. For the liver, tissue composition was measured using an NMR-based analyzer (EchoMRI^{TM}) immediately upon harvest and prior to freezing. ^{3}H-triolein flux was estimated as previously described (Kusminski et al., 2012; Ye et al., 2014).

Liver lipid extraction and quantification

Liver lipid extraction and quantification were performed at the University of Cincinnati Mouse Metabolic Phenotyping Center. Lipids were extracted using the Folch's extraction method as previously described (Folch et al., 1957). Levels of cholesterol, triglycerides, free fatty acids, and phospholipids in each sample were quantified using specific colorimetric assays.

Immunoblotting

Lysates were prepared from snap frozen liver tissues and resolved on a 4-20% Tris-glycine gel as previously described (Emmer et al., 2020). Immunoblots were probed with antibodies against APOB (70R-15771, 1:1000, Fitzgerald Industries International, Acton MA), PCSK9 (ab31762, 1:1000, Abcam, Cambridge UK), LDLR (ab52818, 1:1000, Abcam, Cambridge UK), HSP90 (4877, 1:1000, Cell Signaling Technology, Danvers MA), and GAPDH (ab181602, 1:5000,

Abcam, Cambridge UK). For endoglycosidase H assays, 30 µg of lysate was analyzed as previously described using the above antibodies (Emmer et al., 2018).

Histology

Tissue processing, embedding, sectioning, hematoxylin and eosin (H&E), and picrosirius red staining were performed at the University of Michigan In-Vivo Animal Core (IVAC). Slides were reviewed by an investigator blinded to the genotype.

Analysis of liver mRNA

Liver RNA was isolated from tissue using an RNeasy Plus Mini Kit according to the manufacturer's instructions (74134, Qiagen, Hilden Germany) and reverse transcription was performed using oligo$(dT)_{12\text{-}18}$ primers (18418012, Invitrogen, Waltham MA). Quantitative PCR reactions were performed using Power SYBR Green PCR Master Mix (4367659, Invitrogen, Waltham MA) and primers listed in **Table S.1**. Total *Surf4* mRNA abundance was calculated using data from primers that bind to exon 5 and 6 on the *Surf4* transcript. Abundance of *Surf4* mRNA that contains exon 2 was obtained using primers specific to exon 2 and exon 3 of the transcript. Normalized transcript abundance was calculated by the $2^{-\Delta\Delta Ct}$ method using *Gapdh* and *Rpl37* as housekeeping controls.

Library preparation and next generation sequencing was performed at the University of Michigan Advanced Genomics Core. Demultiplexed fastq files were aligned against the mouse reference genome (GRCm38.92) using STAR (Dobin et al., 2013) and quantified with RSEM (Li & Dewey, 2011). Differential expression analysis was performed by DESeq2 (Love et al., 2014). Sequencing coverage for the *Surf4* transcript was analyzed using the ggsashimi package (Garrido-Martn et al., 2018).

Acute inactivation of hepatic *Surf4* in adult mice

Hepatic *Surf4* was selectively inactivated in adult mice by injection of adeno-associated virus (AAV) delivering a hepatocyte-specific Cre and a guide RNA targeting *Surf4* or *LacZ* (control) into a Cre-dependent spCas9 knockin mice (Platt et al., 2014) as previously described (X. Wang et al., 2021). Blood samples were collected as previously described (X. Wang et al., 2021) and plasma PCSK9 concentrations were measured by the commercial kit (CY-8078 of MBL) according to the manufacturer's protocol.

To deplete *Surf4* mRNA, N-acetylgalactosamine (GalNAc) conjugated siRNA oligos are synthesized to ensure liver targeting. SiRNA targeting murine *Surf4* or GalNAc conjugated siRNA with scrambled sequence (siCTL) were injected into 6 weeks old male mice subcutaneously with concentrations indicated in the figures. Seven days after injection, blood samples were collected by tail vein, and then centrifuged at 6000 rpm, 4℃ for 10 min to harvest plasma. The plasma PCSK9 concentrations were measured by the commercial kit (CY-8078 of MBL) according to the manufacturer's protocol. SiRNA sequences are listed in **Table S.2**.

Acknowledgements

This work was supported by NIH grants R35HL135793 (DG), R01HL148333 (RK), R01HL157062 (RK), and K08HL148552 (BTE); the National Key R&D Program grant 2018YFA0506900 (XWC); the National Science Foundation of China grants 91957119, 91954001, 31571213, and 31521062 (XWC); the American Heart Association Predoctoral Fellowship 20PRE35210706 (VTT); the University of Michigan Rackham Predoctoral Fellowship (VTT). DG is a Howard Hughes Medical Institute Investigator.

Competing interests

None

References

Adams, E. J., Chen, X. W., O'Shea, K. S., & Ginsburg, D. (2014). Mammalian COPII coat component SEC24C is required for embryonic development in mice. *Journal of Biological Chemistry*, *289*(30), 20858--20870. https://doi.org/10.1074/jbc.M114.566687

Belden, W. J. (2001). Role of Erv29p in Collecting Soluble Secretory Proteins into ER-Derived Transport Vesicles. *Science*, *294*(5546), 1528--1531. https://doi.org/10.1126/science.1065224

Benjannet, S., Rhainds, D., Essalmani, R., Mayne, J., Wickham, L., Jin, W., Asselin, M. C., Hamelin, J., Varret, M., Allard, D., Trillard, M., Abifadel, M., Tebon, A., Attie, A. D., Rader, D. J., Boileau, C., Brissette, L., Chrtien, M., Prat, A., & Seidah, N. G. (2004). NARC-1/PCSK9 and its natural mutants: Zymogen cleavage and effects on the low density lipoprotein (LDL) receptor and LDL cholesterol. *Journal of Biological Chemistry*, *279*(47), 48865--48875. https://doi.org/10.1074/jbc.M409699200

Bonifacino, J. S., & Glick, B. S. (2004). The mechanisms of vesicle budding and fusion. *Cell*, *116*(2), 153-166. https://doi.org/10.1016/s0092-8674(03)01079-1

Chang, X., Zhao, Y., Qin, S., Wang, H., Wang, B., Zhai, L., Liu, B., Gu, H.-m., & Zhang, D.-w. (2021). Loss of Hepatic Surf4 Depletes Lipid Droplets in the Adrenal Cortex but Does Not Impair Adrenal Hormone Production. *Frontiers in Cardiovascular Medicine*, *0*, 1613. https://doi.org/10.3389/FCVM.2021.764024

Chapman, M. J., Ginsberg, H. N., Amarenco, P., Andreotti, F., Born, J., Catapano, A. L., Descamps, O. S., Fisher, E., Kovanen, P. T., Kuivenhoven, J. A., Lesnik, P., Masana, L., Nordestgaard, B. G., Ray, K. K., Reiner, Z., Taskinen, M. R., Tokgzoglu, L., Tybjrg-Hansen, A., & Watts, G. F. (2011). Triglyceride-rich lipoproteins and high-density lipoprotein cholesterol in patients at high risk of cardiovascular disease: Evidence and guidance for management. *European Heart Journal*, *32*(11), 1345--1361. https://doi.org/10.1093/eurheartj/ehr112

Chen, X. W., Wang, H., Bajaj, K., Zhang, P., Meng, Z. X., Ma, D., Bai, Y., Liu, H. H., Adams, E., Baines, A., Yu, G., Sartor, M. A., Zhang, B., Yi, Z., Lin, J., Young, S. G., Schekman, R., & Ginsburg, D. (2013). SEC24A deficiency lowers plasma cholesterol through reduced PCSK9 secretion. *eLife*, *2013*(2), 1--23. https://doi.org/10.7554/eLife.00444

Cohen, J., Pertsemlidis, A., Kotowski, I. K., Graham, R., Garcia, C. K., & Hobbs, H. H. (2005). Low LDL cholesterol in individuals of African descent resulting from frequent nonsense mutations in PCSK9. *Nat Genet*, *37*(2), 161-165. https://doi.org/10.1038/ng1509

Dobin, A., Davis, C. A., Schlesinger, F., Drenkow, J., Zaleski, C., Jha, S., Batut, P., Chaisson, M., & Gingeras, T. R. (2013). STAR: Ultrafast universal RNA-seq aligner. *Bioinformatics*, *29*(1). https://doi.org/10.1093/bioinformatics/bts635

Emmer, B. T., Hesketh, G. G., Kotnik, E., Tang, V. T., Lascuna, P. J., Xiang, J., Gingras, A. C., Chen, X. W., & Ginsburg, D. (2018). The cargo receptor SURF4 promotes the efficient cellular secretion of PCSK9. *eLife*, *7*, 1--18. https://doi.org/10.7554/eLife.38839

Emmer, B. T., Lascuna, P. J., Tang, V. T., Kotnik, E. N., Saunders, T. L., Khoriaty, R., & Ginsburg, D. (2020). Murine Surf4 is essential for early embryonic development. *PLoS ONE*, *15*(1). https://doi.org/10.1371/journal.pone.0227450

Folch, J., Lees, M., & Stanley, G. H. S. (1957). A Simple Method for the Isolation and Purification of Total Lipides from Animal Tissues. *Journal of Biological Chemistry*, *226*(1), 497--509. https://doi.org/10.1016/S0021-9258(18)64849-5

Freeze, H. H., & Kranz, C. (2010). *Endoglycosidase and glycoamidase release of N-linked glycans* (Vol. 2010). https://doi.org/10.1002/0471140864.ps1204s62

Garrido-Martn, D., Palumbo, E., & Guig. (2018). ggsashimi: Sashimi plot revised for browser- and annotation-independent splicing visualization. *PLoS Computational Biology*, *14*(8), 1--6. https://doi.org/10.1371/journal.pcbi.1006360

Gomez-Navarro, N., Maldutyte, J., Poljak, K., Peak-Chew, S. Y., Orme, J., Bisnett, B. J., Lamb, C. H., Boyce, M., Gianni, D., & Miller, E. A. (2022). Selective inhibition of protein secretion by abrogating receptor-coat interactions during ER export. *Proc Natl Acad Sci U S A*, *119*(31), e2202080119. https://doi.org/10.1073/pnas.2202080119

Hetz, C., Zhang, K., & Kaufman, R. J. (2020). Mechanisms, regulation and functions of the unfolded protein response. *Nat Rev Mol Cell Biol*, *21*(8), 421-438. https://doi.org/10.1038/s41580-020-0250-z

Ipsen, D. H., Lykkesfeldt, J., & Tveden-Nyborg, P. (2018). Molecular mechanisms of hepatic lipid accumulation in non-alcoholic fatty liver disease. *Cellular and Molecular Life Sciences*, *75*(18), 3313--3327. https://doi.org/10.1007/s00018-018-2860-6

Kolovou, G., Vasiliadis, I., Gontoras, N., Kolovou, V., & Hatzigeorgiou, G. (2015). Microsomal Transfer Protein Inhibitors, New Approach for Treatment of Familial Hypercholesterolemia, Review of the Literature, Original Findings, and Clinical Significance. *Cardiovascular Therapeutics*, *33*(2), 71--78. https://doi.org/10.1111/1755-5922.12105

Kusminski, C. M., Holland, W. L., Sun, K., Park, J., Spurgin, S. B., Lin, Y., Askew, G. R., Simcox, J. A., McClain, D. A., Li, C., & Scherer, P. E. (2012). MitoNEET-driven alterations in adipocyte mitochondrial activity reveal a crucial adaptive process that preserves insulin sensitivity in obesity. *Nature Medicine*, *18*(10), 1539--1551. https://doi.org/10.1038/nm.2899

Li, B., & Dewey, C. N. (2011). RSEM: Accurate transcript quantification from RNA-Seq data with or without a reference genome. *BMC Bioinformatics*, *12*. https://doi.org/10.1186/1471-2105-12-323

Lin, Z., King, R., Tang, V., Myers, G., Balbin-Cuesta, G., Friedman, A., McGee, B., Desch, K., Ozel, A. B., Siemieniak, D., Reddy, P., Emmer, B., & Khoriaty, R. (2020). The Endoplasmic Reticulum Cargo Receptor SURF4 Facilitates Efficient Erythropoietin Secretion. *Molecular and Cellular Biology*, *40*(23). https://doi.org/10.1128/mcb.00180-20

Love, M. I., Huber, W., & Anders, S. (2014). Moderated estimation of fold change and dispersion for RNA-seq data with DESeq2. *Genome Biology*, *15*(12). https://doi.org/10.1186/s13059-014-0550-8

Millar, J. S., Cromley, D. A., McCoy, M. G., Rader, D. J., & Billheimer, J. T. (2005). Determining hepatic triglyceride production in mice: comparison of poloxamer 407 with Triton WR-1339. *Journal of Lipid Research*, *46*(9), 2023--2028. https://doi.org/10.1194/JLR.D500019-JLR200

Miller, E., Antonny, B., Hamamoto, S., & Schekman, R. (2002). Cargo selection into COPII vesicles is driven by the Sec24p subunit. *EMBO Journal*, *21*(22), 6105--6113. https://doi.org/10.1093/emboj/cdf605

Mitrovic, S., Ben-Tekaya, H., Koegler, E., Gruenberg, J., & Hauri, H. P. (2008). The Cargo Receptors Surf4, Endoplasmic Reticulum-Golgi Intermediate Compartment (ERGIC)-53, and p25 Are Required to Maintain the Architecture of ERGIC and Golgi. *Molecular Biology of the Cell*, *19*(5), 1976--1990. https://doi.org/10.1091/mbc.E07-10-0989

Musunuru, K., Chadwick, A. C., Mizoguchi, T., Garcia, S. P., DeNizio, J. E., Reiss, C. W., Wang, K., Iyer, S., Dutta, C., Clendaniel, V., Amaonye, M., Beach, A., Berth, K., Biswas, S., Braun, M. C., Chen, H.-M., Colace, T. V., Ganey, J. D., Gangopadhyay, S. A., Garrity, R., Kasiewicz, L. N., Lavoie, J., Madsen, J. A., Matsumoto, Y., Mazzola, A. M., Nasrullah, Y. S., Nneji, J., Ren, H., Sanjeev, A., Shay, M., Stahley, M. R., Fan, S. H. Y., Tam, Y. K., Gaudelli, N. M., Ciaramella, G., Stolz, L. E., Malyala, P., Cheng, C. J., Rajeev, K. G., Rohde, E., Bellinger, A. M., & Kathiresan, S. (2021). In vivo CRISPR base editing of PCSK9 durably lowers cholesterol in primates. *Nature*, *593*(7859), 429--434. https://doi.org/10.1038/s41586-021-03534-y

Oda, Y., Okada, T., Yoshida, H., Kaufman, R. J., Nagata, K., & Mori, K. (2006). Derlin-2 and Derlin-3 are regulated by the mammalian unfolded protein response and are required for ER-associated degradation. *Journal of Cell Biology*, *172*(3), 383--393. https://doi.org/10.1083/jcb.200507057

Palade, G. (1975). Intracellular aspects of the process of protein synthesis. *Science*, *189*(4200), 347-358. https://doi.org/10.1126/science.1096303

Platt, R. J., Chen, S., Zhou, Y., Yim, M. J., Swiech, L., Kempton, H. R., Dahlman, J. E., Parnas, O., Eisenhaure, T. M., Jovanovic, M., Graham, D. B., Jhunjhunwala, S., Heidenreich, M., Xavier, R. J., Langer, R., Anderson, D. G., Hacohen, N., Regev, A., Feng, G., Sharp, P. A., & Zhang, F. (2014). CRISPR-Cas9 knockin mice for genome editing and cancer modeling. *Cell*, *159*(2), 440-455. https://doi.org/10.1016/j.cell.2014.09.014

Popp, M. W., & Maquat, L. E. (2013). Organizing principles of mammalian nonsense-mediated mRNA decay. *Annu Rev Genet*, *47*, 139-165. https://doi.org/10.1146/annurev-genet-111212-133424

Rashid, S., Curtis, D. E., Garuti, R., Anderson, N. N., Bashmakov, Y., Ho, Y. K., Hammer, R. E., Moon, Y. A., & Horton, J. D. (2005). Decreased plasma cholesterol and hypersensitivity to statins in mice lacking Pcsk9. *Proceedings of the National Academy of Sciences*, *102*(15), 5374--5379. https://doi.org/10.1073/pnas.0501652102

Saegusa, K., Sato, M., Morooka, N., Hara, T., & Sato, K. (2018). SFT-4 Surf4 control ER export of soluble cargo proteins and participate in ER exit site organization. *Journal of Cell Biology*, 1--13.

Shen, Y., Gu, H. M., Zhai, L., Wang, B., Qin, S., & Zhang, D. W. (2022). The role of hepatic Surf4 in lipoprotein metabolism and the development of atherosclerosis in apoE(-/-) mice. *Biochim Biophys Acta Mol Cell Biol Lipids*, *1867*(10), 159196. https://doi.org/10.1016/j.bbalip.2022.159196

Shen, Y., Wang, B., Deng, S., Zhai, L., mei Gu, H., Alabi, A., Xia, X., Zhao, Y., Chang, X., Qin, S., & wei Zhang, D. (2020). Surf4 regulates expression of proprotein convertase subtilisin/kexin type 9 (PCSK9) but is not required for PCSK9 secretion in cultured human hepatocytes. *Biochimica et Biophysica Acta (BBA) - Molecular and Cell Biology of Lipids*, *1865*(2), 158555. https://doi.org/10.1016/J.BBALIP.2019.158555

Tang, A. T., Choi, J. P., Kotzin, J. J., Yang, Y., Hong, C. C., Hobson, N., Girard, R., Zeineddine, H. A., Lightle, R., Moore, T., Cao, Y., Shenkar, R., Chen, M., Mericko, P., Yang, J., Li, L., Tanes, C., Kobuley, D., Vsa, U., Whitehead, K. J., Li, D. Y., Franke, L., Hart, B., Schwaninger, M., Henao-Mejia, J., Morrison, L., Kim, H., Awad, I. A., Zheng, X., & Kahn, M. L. (2017). Endothelial TLR4 and the microbiome drive cerebral cavernous malformations. *Nature*, *545*(7654), 305--310. https://doi.org/10.1038/nature22075

Wang, B., Shen, Y., Zhai, L., Xia, X., Gu, H.-m., Wang, M., Zhao, Y., Chang, X., Alabi, A., Xing, S., Deng, S., Liu, B., Wang, G., Qin, S., & Zhang, D.-w. (2021). Atherosclerosis-associated hepatic secretion of VLDL but not PCSK9 is dependent on cargo receptor protein Surf4. *Journal of Lipid Research*, *62*, 100091. https://doi.org/10.1016/j.jlr.2021.100091

Wang, X., Wang, H., Xu, B., Huang, D., Nie, C., Pu, L., Zajac, G. J. M., Yan, H., Zhao, J., Shi, F., Emmer, B. T., Lu, J., Wang, R., Dong, X., Dai, J., Zhou, W., Wang, C., Gao, G., Wang, Y., Willer, C., Lu, X., Zhu, Y., & Chen, X. W. (2021). Receptor-Mediated ER Export of Lipoproteins Controls Lipid Homeostasis in Mice and Humans. *Cell Metabolism*, *33*(2), 350--366.e357. https://doi.org/10.1016/j.cmet.2020.10.020

Wendeler, M. W., Paccaud, J.-P., Hauri, H.-P., Appenzeller, C., Andersson, H., Kappeler, F., Hauri, H. P., Appenzeller-Herzog, C., Hauri, H. P., Barlowe, C., Barlowe, C., Orci, L., Yeung, T., Hosobuchi, M., Hamamoto, S., Salama, N., Rexach, M. F., Ravazzola, M., Amherdt, M., Schekman, R., Kappeler, F., Klopfenstein, D. R., Foguet, M., Paccaud, J. P., Hauri, H. P., Kim, J., Hamamoto, S., Ravazzola, M., Orci, L., Schekman, R.,

Kurihara, T., Hamamoto, S., Gimeno, R. E., Kaiser, C. A., Schekman, R., Yoshihisa, T., Lee, M. C., Miller, E. A., Goldberg, J., Orci, L., Schekman, R., Miller, E. A., Beilharz, T. H., Malkus, P. N., Lee, M. C., Hamamoto, S., Orci, L., Schekman, R., Mossessova, E., Bickford, L. C., Goldberg, J., Nichols, W. C., Nishimura, N., Balch, W. E., Nufer, O., Guldbrandsen, S., Degen, M., Kappeler, F., Paccaud, J. P., Tani, K., Hauri, H. P., Nufer, O., Kappeler, F., Guldbrandsen, S., Hauri, H. P., Pagano, A., Letourneur, F., Garcia-Estefania, D., Carpentier, J. L., Orci, L., Paccaud, J. P., Peng, R., Antoni, A. D., Gallwitz, D., Shimoni, Y., Kurihara, T., Ravazzola, M., Amherdt, M., Orci, L., Schekman, R., Tang, B. L., Kausalya, J., Low, D. Y., Lock, M. L., Hong, W., Vollenweider, F., Kappeler, F., Itin, C., & Hauri, H. P. (2007). Role of Sec24 isoforms in selective export of membrane proteins from the endoplasmic reticulum. *EMBO reports*, *8*(3), 258--264. https://doi.org/10.1038/sj.embor.7400893

Ye, R., Holland, W. L., Gordillo, R., Wang, M., Wang, Q. A., Shao, M., Morley, T. S., Gupta, R. K., Stahl, A., & Scherer, P. E. (2014). Adiponectin is essential for lipid homeostasis and survival under insulin deficiency and promotes β-cell regeneration. *eLife*, *3*, 1--21. https://doi.org/10.7554/eLife.03851

Yin, Y., Garcia, M. R., Novak, A. J., Saunders, A. M., Ank, R. S., Nam, A. S., & Fisher, L. W. (2018). Surf4 (Erv29p) binds amino-terminal tripeptide motifs of soluble cargo proteins with different affinities, enabling prioritization of their exit from the endoplasmic reticulum. *PLoS Biology*, *16*(8), e2005140. https://doi.org/10.1371/journal.pbio.2005140

Table 1: Genotype distribution of offspring of *Surf4$^{fl/fl}$ Alb-Cre^{+}* and *Surf4$^{fl/+}$ Alb-Cre^{-}* intercrosses

Genotype (Expected)	***Surf4$^{fl/+}$ Alb-Cre^{-}*** **(25%)**	***Surf4$^{fl/+}$ Alb-Cre^{+}*** **(25%)**	***Surf4$^{fl/fl}$ Alb-Cre^{-}*** **(25%)**	***Surf4$^{fl/fl}$ Alb-Cre^{+}*** **(25%)**	***p* (χ^2)**
Mating	♂ *Surf4$^{fl/fl}$ Alb-Cre^{-}* X ♀ *Surf4$^{fl/+}$ Alb-Cre^{+}*				
	61 (25.8%)	71 (30.1%)	60 (25.4%)	44 (18.6%)	0.096
Mating	♂ *Surf4$^{fl/+}$ Alb-Cre^{-}* X ♀ *Surf4$^{fl/fl}$ Alb-Cre^{+}*				
	8 (18.6%)	9 (20.9%)	12 (27.9%)	14 (32.6%)	0.549

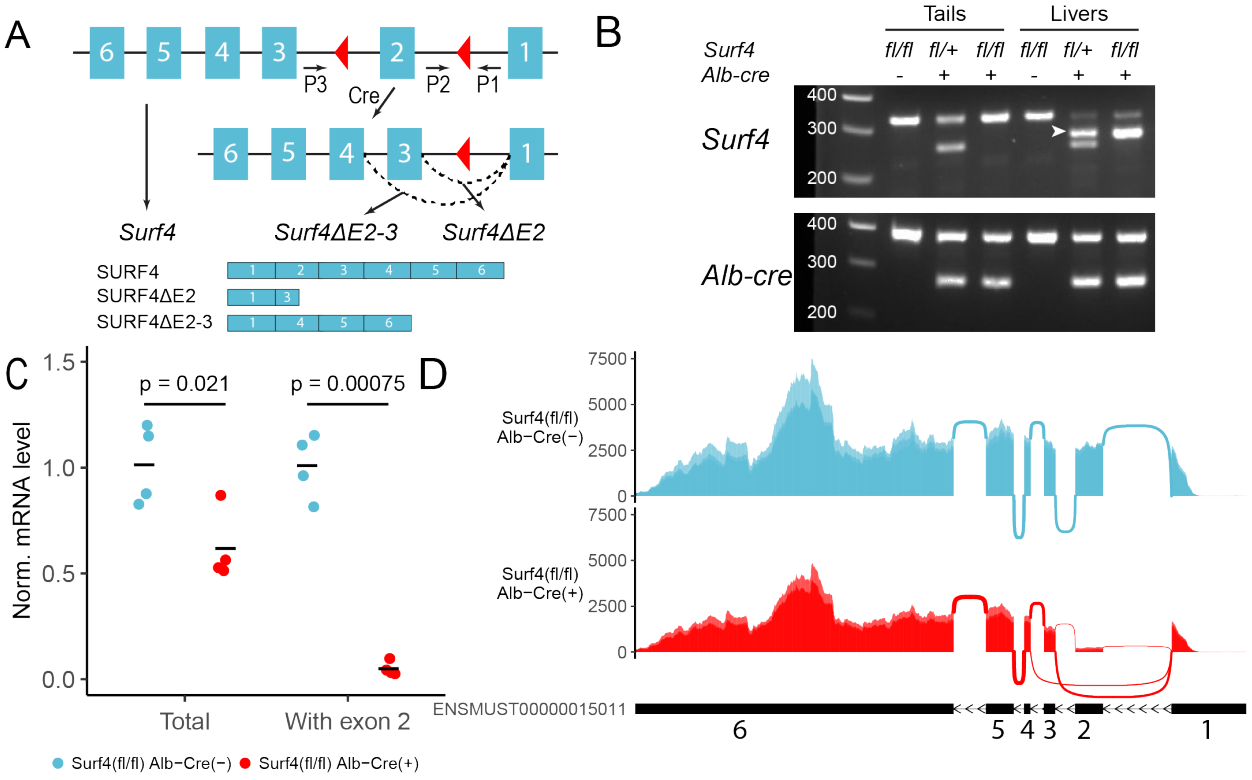

Figure 1. Generation of hepatocyte-specific *Surf4* deficient mice. (A) Schematic presentation of the *Surf4* conditional allele. Blue rectangles represent exons and black line segments represent introns. Red triangles denote loxP sites. Expression of a *Cre* recombinase leads to excision of exon 2, which results in the generation of a *Surf4* mRNA lacking exon 2 (*Surf4ΔE2)* or both exon 2 and 3 (*Surf4ΔE2-3*). *Surf4ΔE2* mRNA is translated into a truncated SURF4 that is only 22 amino acids in length. *Surf4ΔE2-3* mRNA restores the reading frame, producing an internally truncated protein missing the 88 amino acids encoded by exon 2 and 3. P1, P2, P3 indicate the positions for *Surf4* genotyping primers. Dashed lines represent splicing events. Exons and introns are not drawn to scale. **(B)** Agarose gel electrophoresis of PCR products generated using genomic DNA (gDNA) isolated from mouse tails and livers and primers P1-3 shown in (A). For *Surf4* genotyping, the wild type allele produces a smaller PCR product whereas the conditional allele produces a larger amplicon. Excision of exon 2 results in the generation of a PCR product of intermediate size (white arrowheads) that is present in

gDNA isolated from the livers of *Alb-Cre*$^{+}$ mice only. For *Alb-Cre* genotyping, presence of the *cre* transgene results in a smaller PCR product. The upper band represents the amplification of an internal control. **(C)** Quantification of Normalized (Norm.) *Surf4* mRNA abundance by quantitative PCR of liver cDNA from control (*Surf4*$^{fl/fl}$ *Alb-Cre*$^{-}$) and *Surf4*$^{fl/fl}$ *Alb-Cre*$^{+}$ mice. Crossbars represent the mean normalized abundance in each group. The denoted p-value was calculated by two-sided Student's t-test. **(D)** Density plots of RNA-seq reads mapping along exon and exon-exon junctions of *Surf4* mRNA. *Surf4*$^{fl/fl}$ *Alb-Cre*$^{+}$ samples have lower read counts due to incomplete nonsense mediated mRNA decay. Arcs between exons represent splicing events and line thickness is proportional to read count. Exact read counts are presented in figure S.1.

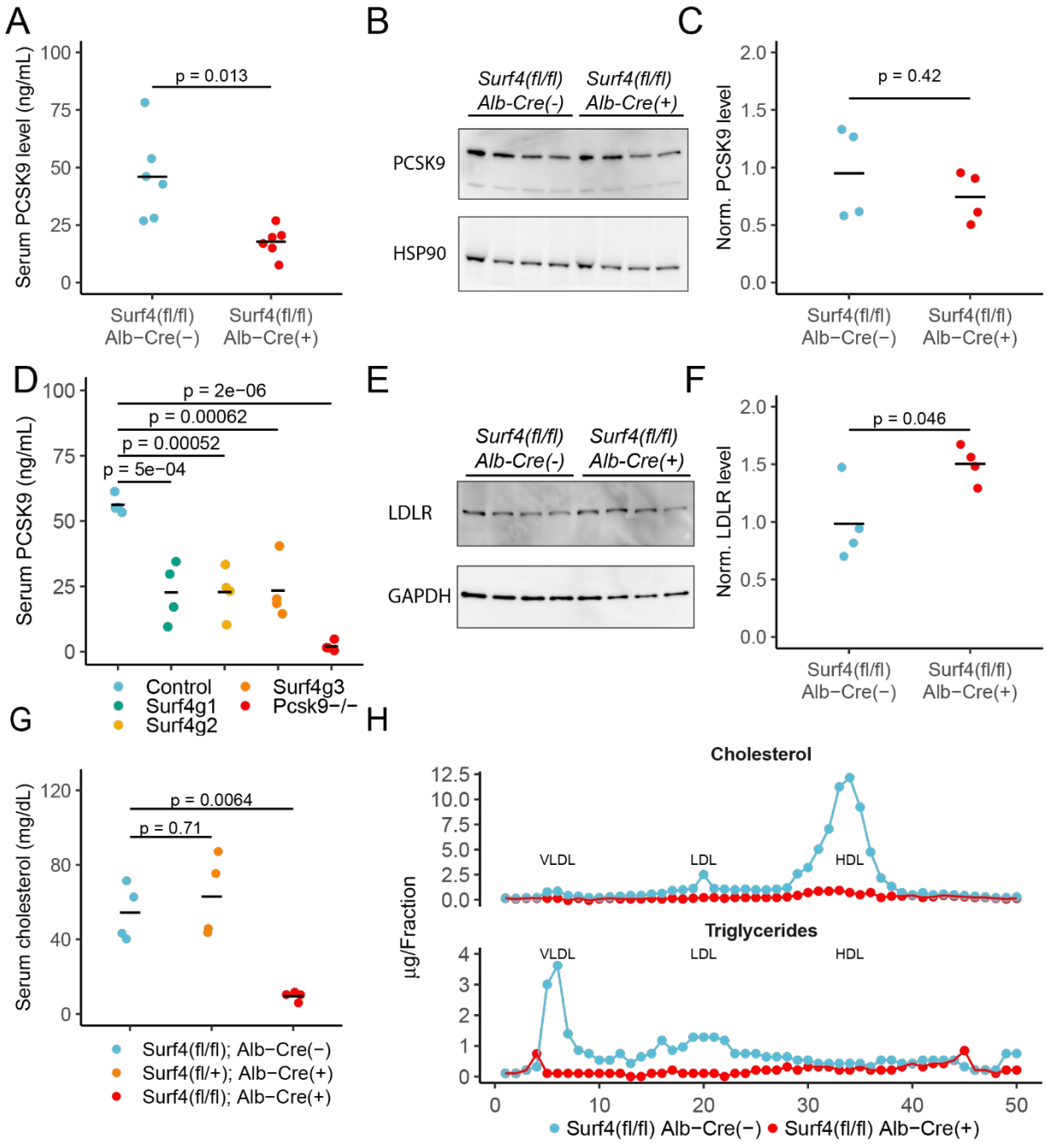

Figure 2. Deletion of hepatic *Surf4* results in decreased serum PCSK9 level and profound hypocholesterolemia in mice. (A) Serum PCSK9 levels measured by ELISA in *Surf4*$^{fl/fl}$ *Alb-Cre*$^{+}$ mice and *Surf4*$^{fl/fl}$ *Alb-Cre*$^{-}$ littermate controls. **(B)** Immunoblot for PCSK9 and HSP90 (loading control) in liver lysates collected from control and *Surf4*$^{fl/fl}$ *Alb-Cre*$^{+}$ mice. **(C)** Quantification of liver PCSK9 levels presented in (B). **(D)** Serum PCSK9 levels in mice in which

hepatic *Surf4* was acutely inactivated by CRISPR/Cas9. **(E)** Immunoblot of liver lysates collected from control and *Surf4*$^{fl/fl}$ *Alb-Cre*$^{+}$ mice for LDLR and GAPDH (loading control). **(F)** Quantification of liver LDLR levels presented in (E). **(G)** Steady-state plasma cholesterol levels in 2 months old control (*Surf4*$^{fl/fl}$ *Alb-Cre*$^{-}$), heterozygous (*Surf4*$^{fl/+}$ *Alb-Cre*$^{+}$), and homozygous (*Surf4*$^{fl/fl}$ *Alb-Cre*$^{+}$) mice. **(H)** Fractionation of lipoproteins in mouse serum by fast protein liquid chromatography (FPLC). Cholesterol and triglyceride levels were measured in each fraction. Each control and *Surf4*$^{fl/fl}$ *Alb-Cre*$^{+}$ sample was pooled from sera of 5 mice. Fractions corresponding to VLDL, LDL, and HDL are annotated. Crossbars represent the mean in all plots. For comparisons between control and *Surf4*$^{fl/fl}$ *Alb-Cre*$^{+}$, p-values were calculated by two-sided Student's t-test. For comparison between control, heterozygous, and *Surf4*$^{fl/fl}$ *Alb-Cre*$^{+}$, p-value were obtained by one-way ANOVA test followed by Tukey's post hoc test.

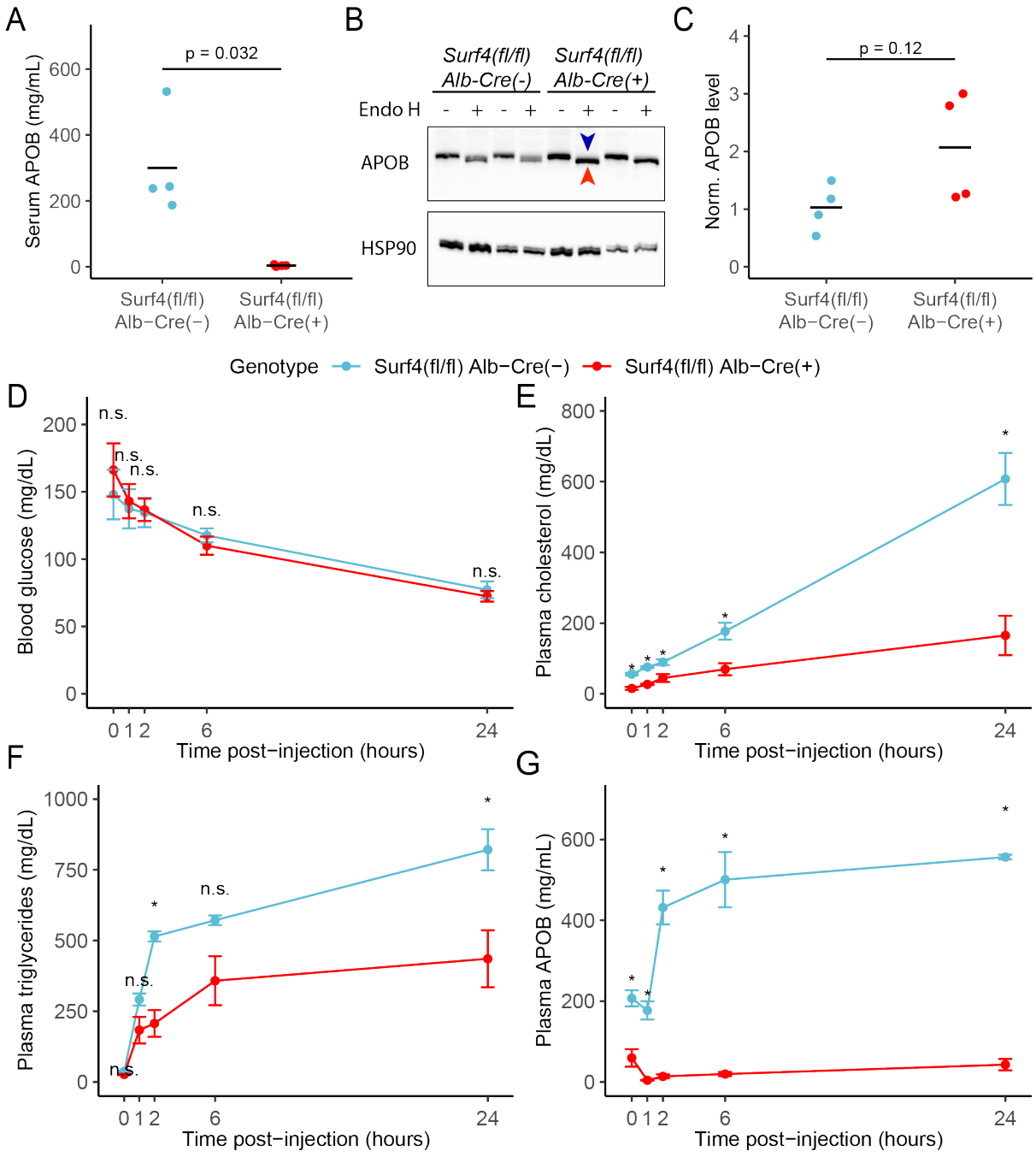

Figure 3. Hepatic lipoprotein and APOB secretion defect in *Surf4*$^{fl/fl}$ *Alb-Cre*$^{+}$ mice. (A) Steady-state serum APOB levels in control and *Surf4*$^{fl/fl}$ *Alb-Cre*$^{+}$ mice at 2 months of age. **(B)** Representative immunoblot for APOB and HSP90 in liver lysates with and without endoglycosidase H (endo H) treatment. Proteins in the pre-Golgi compartments are expected to be sensitive to endo H cleavage, resulting in an electrophoretic shift on an immunoblot. Blue

arrowhead indicates the endo H resistant band whereas the red arrowhead indicates the endo H sensitive band. Accumulation of endo H sensitive SURF4 suggests accumulation in the ER. **(C)** Quantification of APOB abundance in control and *Surf4*$^{fl/fl}$ *Alb-Cre*$^{+}$ liver lysates, without endo H treatment. For panel A and C, crossbars represent the mean, with statistical significance determined by two-sided Student's t-test. **(D-G)** *Surf4*$^{fl/fl}$ *Alb-Cre*$^{+}$ and littermate control mice were injected with a lipoprotein lipase inhibitor to block triglyceride hydrolysis. Blood was sampled prior to and following injection over 24 hours and assayed for **(D)** glucose, **(E)** cholesterol, **(F)** triglycerides, and **(G)** APOB levels. Data are presented as mean ± SEM for each time point (n=5 per group). Asterisks denotes $p < 0.05$ obtained from two-sided Student's t-test with Benjamini-Hochberg adjustment for multiple hypothesis testing, n.s., not significant.

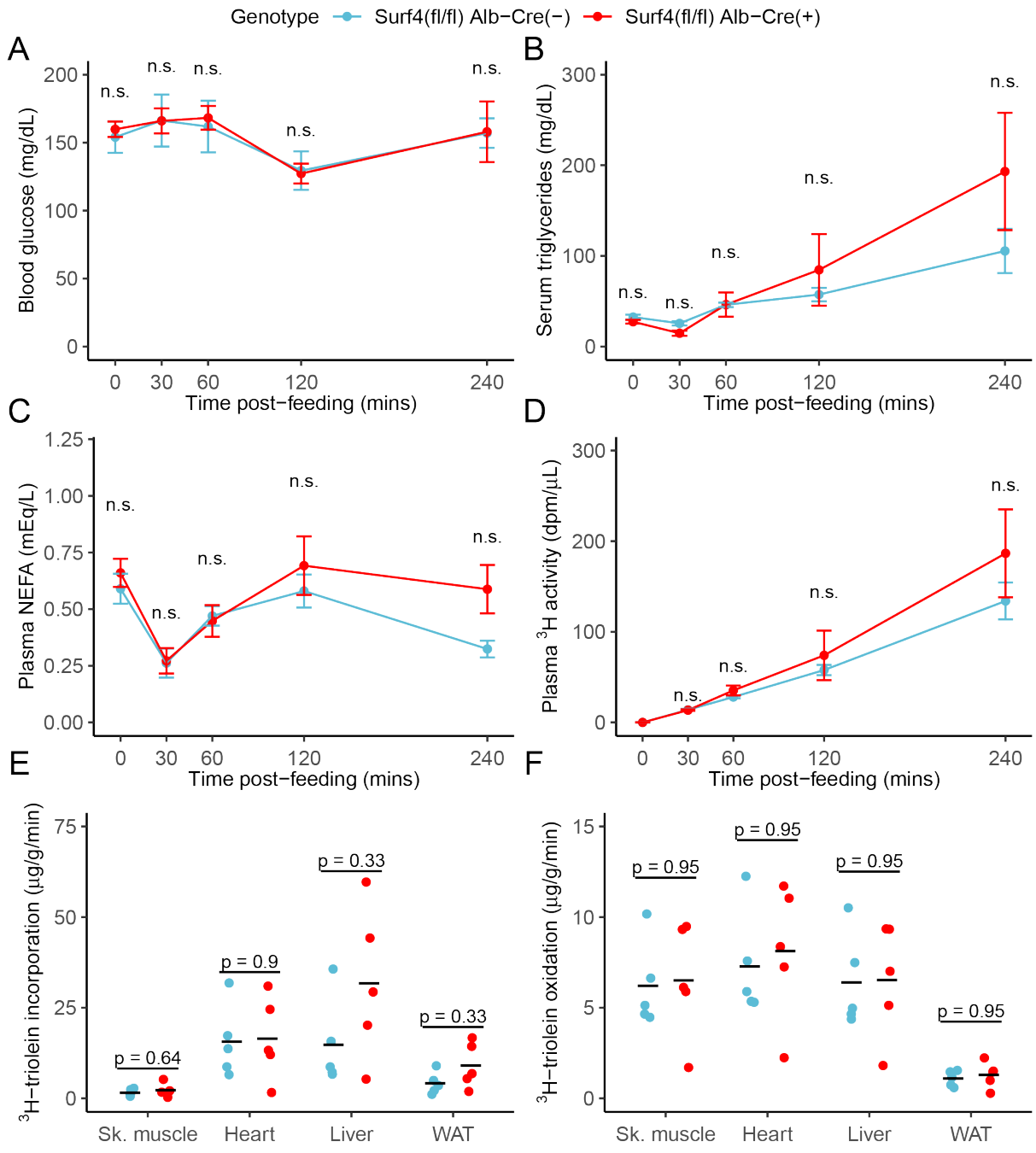

Figure 4. Inactivation of hepatic *Surf4* does not impact dietary lipid absorption, incorporation, and oxidation. Mice were administered ^{3}H-labelled triolein by oral gavage. Blood samples were collected over 4 hours and assayed for **(A)** glucose, **(B)** triglycerides, **(C)** non-esterified fatty acids (NEFA), and **(D)** ^{3}H radioactivity. Data are presented as mean ± SEM for each time point (n=5 per group), n.s., not significant. **(E-F)** Tissues were collected at the 4

hour time point and lipids were extracted by the Folch's method. ^{3}H radioactivity was measured in the hydrophobic phase, which represents incorporated triolein **(E)** and hydrophilic phase, which represents oxidized triolein **(F)**. All crossbars represent the mean. The denoted p-values were obtained by two-sided Student's t-test with Benjamini-Hochberg adjustment for multiple hypothesis testing.

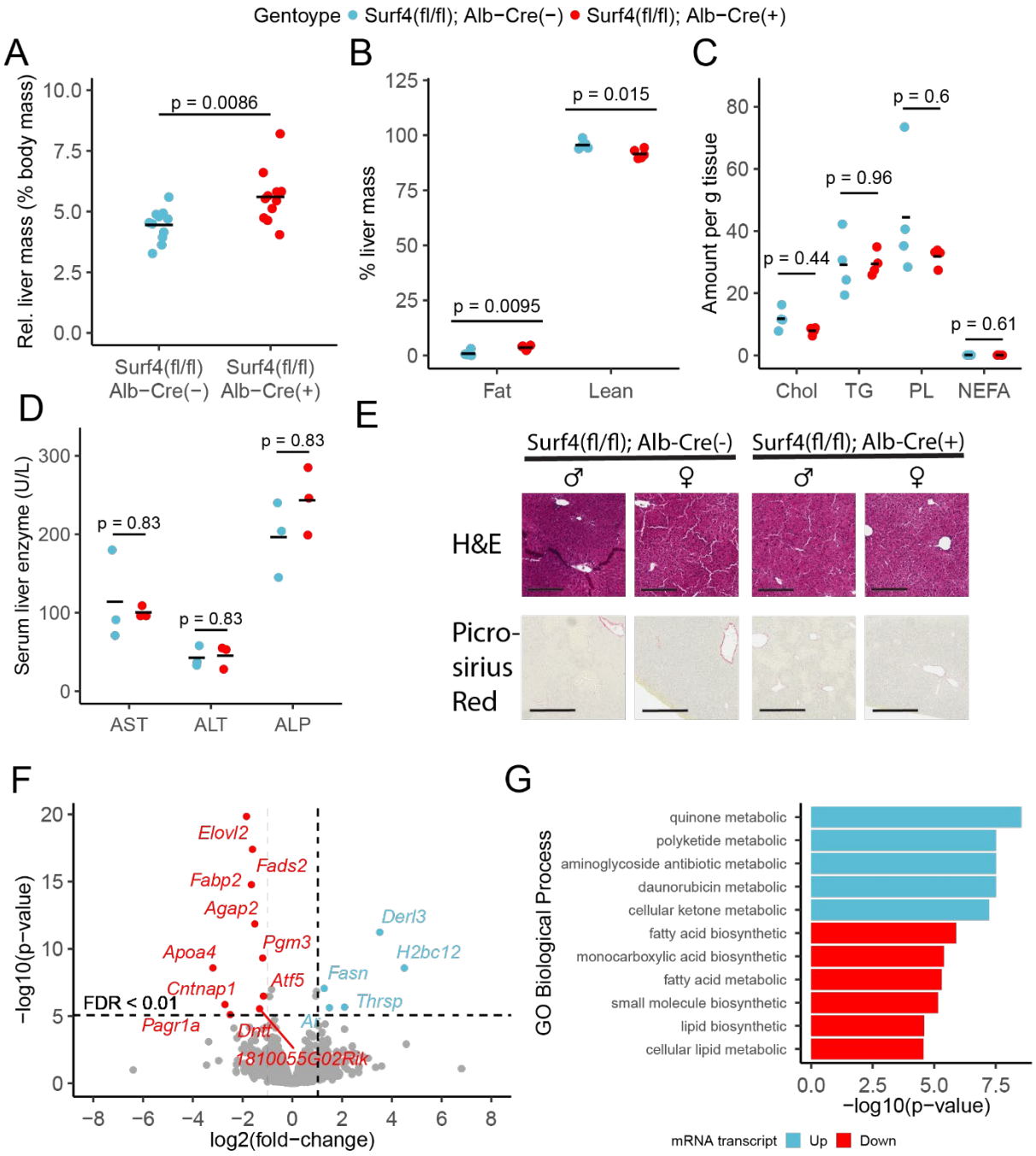

Figure 5. Hepatic *Surf4* deletion results in mild hepatomegaly and an increase in liver lipid content, without apparent liver dysfunction or steatohepatitis. (A) Relative liver mass in control and *Surf4*$^{fl/fl}$ *Alb-Cre*$^{+}$ mice presented as percentage of total body mass. **(B)** Relative fat and lean mass in the livers of control and *Surf4*$^{fl/fl}$ *Alb-Cre*$^{+}$ mice measured by EchoMRI™ and presented as percentage of liver mass. **(C)** Levels of cholesterol (Chol, mg/g tissue),

triglycerides (TG, mg/g tissue), phospholipids (PL, mg/g tissue), and nonesterified fatty acid (NEFA, mEq/g tissue) in lipids extracted from the livers. **(D)** Serum levels of asparate aminotransferase (AST), alanine transaminase (ALT), and alkaline phosphatase (ALP). **(E)** H&E and picrosirius red stained liver sections from control and *Surf4*$^{fl/fl}$ *Alb-Cre*$^{+}$ mice. Scale bars represent 200 μm in H&E images and 300 μm in picrosirius red images. **(F)** Changes in mRNA transcript levels in *Surf4*$^{fl/fl}$ *Alb-Cre*$^{+}$ mice compared to littermate controls. Horizontal line represents the p-value above which the false discovery rate (FDR) is less than 0.01. Significantly up (blue) or down (red) regulated transcripts are labelled. **(G)** Significantly overrepresented Gene Ontology (GO) terms for biological processes in up and down regulated gene lists. For panels A-D: All crossbars represent the mean. P-values were obtained by two-sided Student's t-test with Benjamini-Hochberg adjustment for multiple hypothesis testing where appropriate.

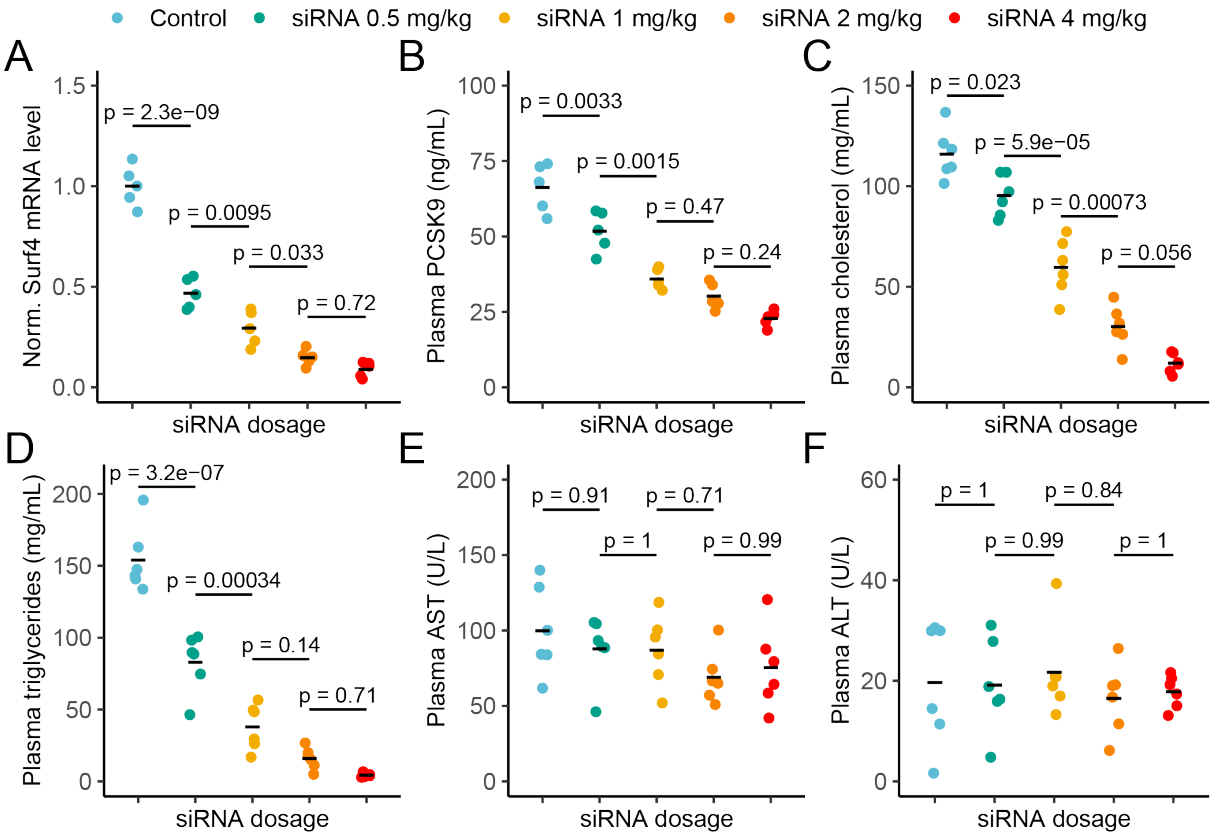

Figure 6. Depletion of hepatic *Surf4* by siRNA recapitulates the hypolipidemia seen in *Surf4*$^{fl/fl}$ *Alb-Cre*$^{+}$ mice. (A) Relative liver *Surf4* mRNA levels in mice treated with scrambled siRNA (control) or varying concentrations of *Surf4* targeting siRNA. **(B-D)** Plasma PCSK9, cholesterol, and triglyceride levels in control and siRNA treated mice. **(E-F)** Plasma levels of asparate aminotransferase (AST) and alanine transaminase (ALT) in mice treated with control or increasing doses of *Surf4* targeting siRNA. Statistical significance was computed by one-way ANOVA test followed by Tukey's post hoc test.

Table S.1. Primers used in this study

Primer name	Target	Sequence (5' → 3')
Surf4-fl-F1 (P1)	*Surf4*	TGAGAAAAGTATGGAGTCCACCTGC
Surf4-fl-R1 (P2)	*Surf4*	AACAGCTGTGCTATGGGCTGGAAAG
Surf4-fl-R2 (P3)	*Surf4*	CCTGCCTCTAAATCCCAAATGCTGTCG
Cre-genotyping-F1	*Cre transgene*	CCATCTGCCACCAGCCAG
Cre-genotyping-R1	*Cre transgene*	TCGCCATCTTCCAGCAGG
Cre-genotyping-F2	*Cpxm1* (Control)	ACTGGGATCTTCGAACTCTTTGGAC
Cre-genotyping-R2	*Cpxm1* (Control)	GATGTTGGGGCACTGCTCATTCACC
Alb-cre-F1	*Alb-Cre*	TGCAAACATCACATGCACAC
Alb-cre-R1	*Alb-Cre*	TTGGCCCCTTACCATAACTG
Alb-cre-R2	*Alb-Cre*	GAAGCAGAAGCTTAGGAAGATGG
Surf4-qPCR-F1	*Surf4* (exon 2)	CTGTTGGCCTCATCCTTCGT
Surf4-qPCR-R1	*Surf4* (exon 3)	GGCAATTGTCTGCAGTGCG
Surf4-qPCR-F2	*Surf4* (exon 5)	TTTGCTGGTGTCCCAACCAT
Surf4-qPCR-R2	*Surf4* (exon 6)	AGCTGTGCCCACAATGTTCT
Pcsk9-qPCR-F1	*Pcsk9*	TATAGCCGCATCCTCAACGC
Pcsk9-qPCR-R1	*Pcsk9*	CCCGACTGTGATGACCTCTG
Rpl37-F	*Rpl37*	CGGGACTGGTCGGATGAG
Rpl37-R	*Rpl37*	TCACGGAATCCATGTCTGAATC
Gapdh-F	*Gapdh*	ACCCAGAAGACTGTGGATGG
Gapdh-R	*Gapdh*	ACACATTGGGGGTAGGAACA

Table S.2. Sequences and modifications of oligonucleotides for siRNA in mice

	Sense (5'-3') 3' GalNAc conjugated	Antiense (5'-3') 3' GalNAc conjugated
si*Surf4*-1	CmsCmsAmUmCfAmAfCfGfUmGmUm AmUmUmUmCmAmAm	UmsUfsGmAmAmAfUmAfCfAmCmGm UmUfGmAfUmGmGmsCmsAm
si*Surf4*-2	GmsGmsAmCmAfAmUfCfCfCmGmGm UmAmUmAmUmAmAm	UmsUfsAmUmAmUfAmCfCfGmGmGm AmUfUmGfUmCmCmsAmsGm
siCTL	mU*mU*mCmUfCmCfGfAfAmC mGmUmGmUmCmAmCmGmU	mA*fC*mGmUmGfAmCfAfCmGmUmU mCfGmGfAmGmAmA*mU*mU

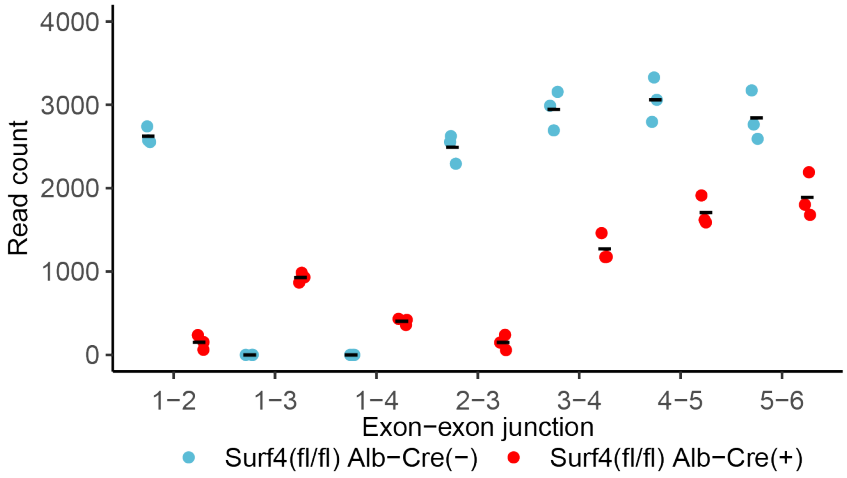

Figure S.1. Read counts mapping to exon-exon junctions along the *Surf4* transcript based on RNA-sequencing data.

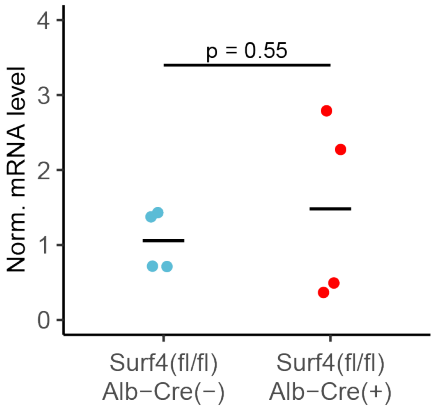

Figure S.2. Normalized (Norm.) *Pcsk9* mRNA levels in *Surf4*$^{fl/fl}$ *Alb-Cre*$^{-}$.and *Surf4*$^{fl/fl}$ *Alb-Cre*$^{+}$ livers. Crossbars represent the mean, p-values were obtained from a two-sided Student's t-test.

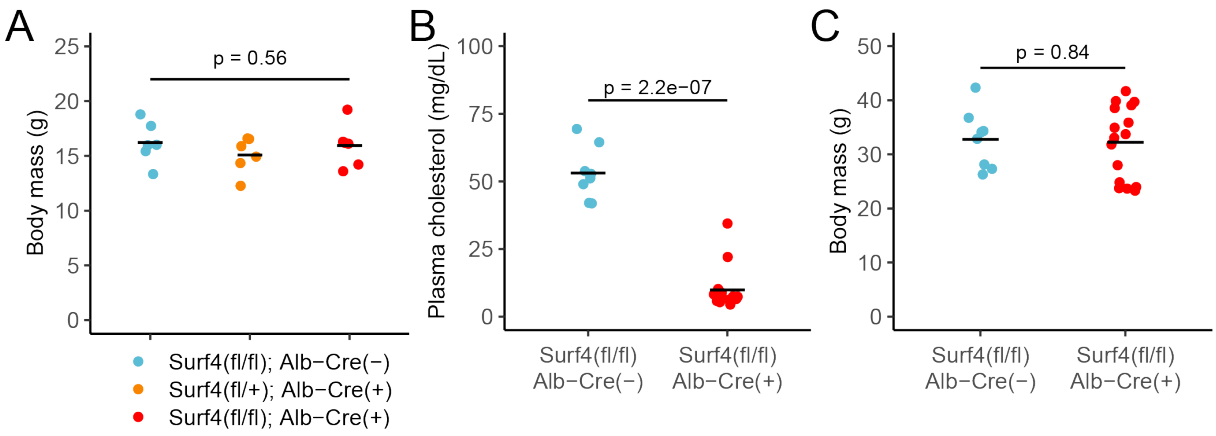

Figure S.3. (A) Body mass of control (*Surf4*$^{fl/fl}$ *Alb-Cre*$^{-}$), heterozygous (Het, *Surf4*$^{fl/+}$ *Alb-Cre*$^{+}$), and homozygous (*Surf4*$^{fl/fl}$ *Alb-Cre*$^{+}$) mice at 2 months of age. P-value was obtained by a one-way ANOVA test. **(B-C)** Serum cholesterol and body mass of 1 year old control and *Surf4*$^{fl/fl}$ *Alb-Cre*$^{+}$ mice. P-values were obtained from a two-sided Student's t-test. For all panels: crossbars represent the mean.

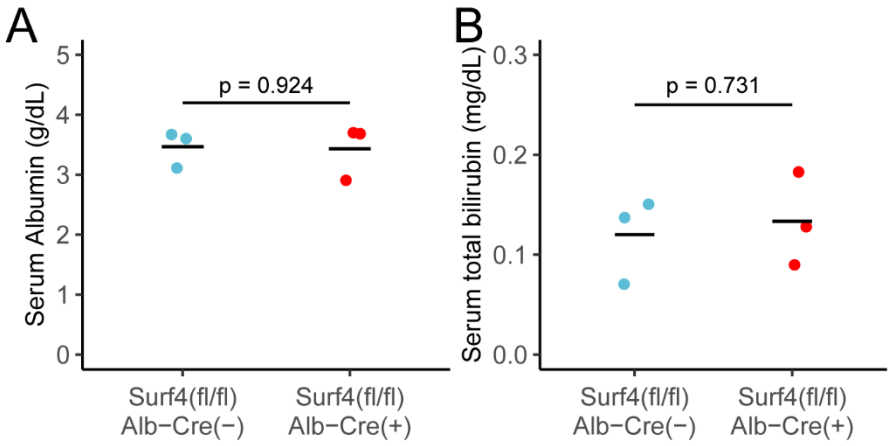

Figure S.4. Serum **(A)** albumin and **(B)** bilirubin levels in *Surf4*$^{fl/fl}$ *Alb-Cre*$^{-}$ and *Surf4*$^{fl/fl}$ *Alb-Cre*$^{+}$ mice. Crossbars represent the mean. P-values were obtained from two-sided Student's t-test.

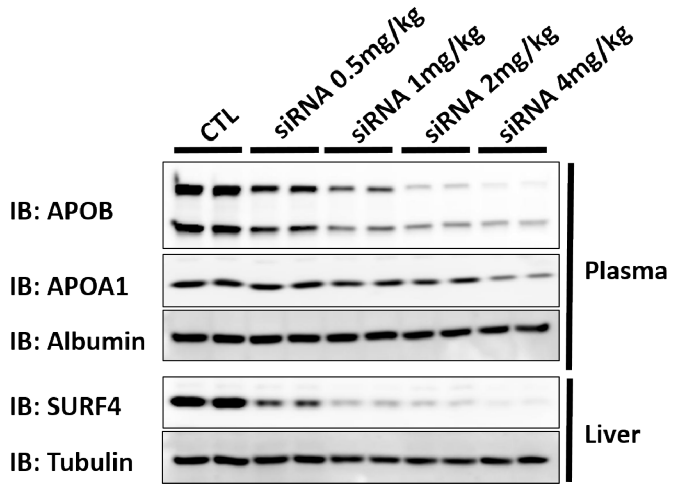

Figure S.5. Immunoblot of plasma and liver lysates collected from mice treated with control or increasing doses of *Surf4* targeting siRNA.